

Article

# Aluminum Particle Ignition Studies with Focus on Effect of Oxide Barrier

Nadir Yilmaz <sup>1,\*</sup>, Burl Donaldson <sup>2</sup> and Walt Gill <sup>2</sup><sup>1</sup> Department of Mechanical Engineering, Howard University, Washington, DC 20059, USA<sup>2</sup> Sandia National Laboratories, Albuquerque, NM 87123, USA

\* Correspondence: nadir.yilmaz@howard.edu; Tel.: +1-2028066600

**Abstract:** Aluminum particle ignition behavior in open atmosphere rocket propellants fires is of particular interest for preventing accidents for rockets carrying high-value payloads. For nominal motor pressures, aluminum particles oxidize to aluminum oxide in the gas phase and release significant combustion energy while minimizing motor instability. During rocket abort or launch pad malfunction which occur under atmospheric or low pressure, behavior of aluminum particle combustion becomes complex and aluminum appears to melt, agglomerate or form a skeletal structure. Furthermore, an oxide shell of alumina instantly forms on any fresh aluminum surface which is exposed to an oxidizing environment. Aluminum combustion then strongly depends on the oxide layer growth, which is influenced by causative factors, including particle size, environmental gas composition, and heating rate. This work focuses on the effect of the oxide barrier which forms on the surface of aluminum that is recognized to impede combustion of aluminum in solid rocket propellants. Understanding the mechanism for breach of this barrier is deemed to be an important consideration in the overall process. In this discussion, results of various experiments will be discussed which have a bearing on this process. Basically, a recognized criterion is the melting of the oxide layer at 2350 K is sufficient. However, in other situations, depending on the mechanism of oxide formation, there will occur defects in the oxide shell which provide for aluminum ignition at lower temperatures. For slow heating in an oxidizing environment, where the oxide layer can grow thick, then ignition is more difficult. Because there is no uniform model to establish an ignition criterion due to the unknown history of an aluminum particle, this paper reports experimental findings involving oxyacetylene torch, thermogravimetric analysis with differential scanning calorimeter, aluminum particle heating, electric ignition and aluminum powder heating, to address the influence of the oxide layer on the aluminum particle ignition.

**Keywords:** aluminum; particle ignition; combustion; oxide layer; rocket propulsion; solid propellant



**Citation:** Yilmaz, N.; Donaldson, B.; Gill, W. Aluminum Particle Ignition Studies with Focus on Effect of Oxide Barrier. *Aerospace* **2023**, *10*, 45. <https://doi.org/10.3390/aerospace10010045>

Academic Editor: Konstantinos Kontis

Received: 6 November 2022

Revised: 20 December 2022

Accepted: 23 December 2022

Published: 3 January 2023



**Copyright:** © 2023 by the authors. Licensee MDPI, Basel, Switzerland. This article is an open access article distributed under the terms and conditions of the Creative Commons Attribution (CC BY) license (<https://creativecommons.org/licenses/by/4.0/>).

## 1. Introduction

In consideration of the thermal environment to which a solid propellant rocket payload might be exposed in the event of an abort fire, the behavior of aluminum powder as a propellant component is potentially a significant consideration. Aluminum particles oxidize to aluminum oxide (alumina,  $Al_2O_3$ ) in the gas phase under high rocket motor pressures which lead to more stable combustion in the rocket motor. However, for low or atmospheric pressure combustion, which would be expected during rocket abort or launch pad malfunction, the outcome is not clear [1–3]. For example, in low pressure strand burner measurements for some propellants, aluminum appears to melt, agglomerate and either form a skeletal structure mimicking the original shape, or collect in the bottom of the chamber as essentially free aluminum. However, in testing with larger samples of aluminized propellant, production of white smoke is observed, indicative of aluminum oxidation, even though unburned aluminum deposits may be found on the floor of the test cell afterwards. In order to support the modeling of solid propellant fires and the attendant

heat flux, it is necessary to improve understanding of the mechanisms and conditions under which aluminum particles may ignite and burn, thus contributing to the heat load on an exposed object.

The issue of uncertainty in aluminum powder participation in atmospheric pressure solid propellant combustion was raised in some early Sandia National Labs (SNL) studies of various propellant formulations [4]. Heat flux measurements were made and results compared to a model based on the calculated adiabatic flame temperature which assumed equilibrium oxidation of aluminum. Results indicated that the discrepancy between measurements and the model was greatest when the aluminum loading in the propellant was highest. In other words, the assumption of equilibrium oxidation of aluminum was deemed to be suspect.

The aluminum oxide, often referred to as alumina, is the layer that covers pure aluminum giving the aluminum a shiny sheen. It is an accepted notion among researchers who deal with aluminum combustion that an alumina barrier coating will be quickly established with a layer of alumina  $\approx 4$  nm thick forming in about 100 picoseconds on any surface of exposed aluminum. This occurs because aluminum is very reactive with oxygen in the atmosphere. This oxide layer acts as a protective shield around the aluminum particle keeping it from further reaction with the outside atmosphere. This is problematic where aluminum particles are used in rocketry since this layer has a high melting point keeping the pure aluminum within from igniting and restricting or not allowing combustion to occur. The thickness of the alumina shell or barrier can depend on several factors, including time of exposure, temperature, and the oxygen concentration of the environment [5,6]. Later discussion appears to lead to the conjecture that the barrier coating is not uniform and may have defects of unknown origin, perhaps during original synthesis of powder from an aluminum billet. Literature deals with conditions for the ignition of aluminum under various stimuli, with emphasis on the role of the oxide layer and its relationship to outcome.

Friedman and Macek [7] studied ignition by dropping single aluminum particles into hot gases and confirmed the generally accepted opinion that ignition occurs only when the ambient gases are sufficiently hot that the melting point of alumina is reached, i.e., near 2300 K, so that aluminum vapor can escape from the droplet and come into intimate contact with oxidizing gas. They noted some limited ignition dependence on oxygen composition of the gases and aluminum particle size. They did observe particle fragmentation when the free oxygen mole fraction in the combustion gases exceeded 0.26 and the gas temperature was above 2250 K, whereas when there was a deficit of free oxygen in the surrounding gas, the required ignition temperature approached 2370 K.

Gal'chenko et al. [8] studied aluminum ignition by electrically heating wire in a flowing stream of carbon dioxide and contrasted these results with their earlier work where pure oxygen was the flowing gas. They found that in pure oxygen, the oxide layer becomes much thicker during the induction period, but that the ignition temperature can be lower than the melting point of  $\text{Al}_2\text{O}_3$  by as much as 400 K. However, for carbon dioxide, achieving the melting temperature of alumina was a necessary condition for ignition.

Price et al. [9] extensively studied aluminum combustion and report on a major study for the Air Force Office of Scientific Research related to the behavior of aluminum powder in burning ammonium perchlorate propellant. The major focus was to identify the process of aluminum ignition using high speed photography to observe phenomena and much of this work was carried out at high pressure. However, since pressure was a variable in many of the experiments, then atmospheric pressure testing was frequently included. This research employed high magnification along with high-speed photography of the burning propellant surface. Although Price acknowledges several routes to aluminum oxidation, the typical route is described thusly: "aluminum concentrates on the burning surface (propellant surface), agglomerates, ignites and detaches from the surface as a single complex event; burns as 50–300  $\mu\text{m}$  agglomerates while moving away from the burning surface; forms a fine  $\text{Al}_2\text{O}_3$  smoke in a flame envelope about the agglomerate; concurrently accumulates oxide on the surface of agglomerates that end up as residual

oxide droplets in the 5–100  $\mu\text{m}$  range when the agglomerates burn out". Elaborating on this description: "low volatility of the metal, protective nature of the oxide skin, and initially low local concentration of oxidizing species prevent ignition of the metal during this surface (propellant surface) accumulation; such accumulation occurs without ignition even on the burning surface of the AP (ammonium perchlorate) propellant". Results of their low pressure tests support Price's assertion that because of fall-off in temperature away from the burning surface, the agglomerate temperature may fall below the oxide freezing point which arrests combustion. In fact, from atmospheric pressure testing of a particular propellant, it was found that only around 55% of the aluminum oxidized. Price goes on to report that SEM examination of quenched agglomerates found voids which were noted to be larger in low pressure tests, compared to around 15% void, noted in high pressure tests. An oxide lobe was also observed to form on the agglomerates.

Parr et al. [10] have worked extensively in the area of combustion of a single particle of aluminum (210  $\mu\text{m}$  diameter). In the apparatus used, any native oxide layer was destroyed by pulse laser heating, and Parr notes that oxide lobes reported by others were not seen in these experiments. Since the objective was to study the combustion of a single particle, and not the ignition process, the laser energy deposited in the particle exceeded the minimum ignition threshold. Interesting information and findings from this work include a proposed reaction mechanism, measurement of droplet surface temperatures of approximately 2350 K (corresponding roughly to the melting point of alumina, but a bit lower than the normal boiling point of aluminum) and measurement of maximum gas phase temperature of approximately 3800 K at between  $5\times$  and  $6\times$  the particle radius, which is noted to exceed the calculated adiabatic combustion temperature by around 300 K. Maximum AIO concentration was found to be located at approximately  $2.5\times$  the particle radius and maximum  $\text{Al}_2\text{O}_3$  was found to be located at around  $3.5\times$  particle radius. Parr also noted a two-stage combustion process, wherein the first stage appears to be steady combustion in the gas phase followed by a violent, unsteady burning phase where gaseous ejections from the particle surface were observed.

Dreizin studied aluminum combustion over several years beginning in 1994. In references [11,12], a novel micro-arc (GEMMED) was employed to study combustion of 85–190  $\mu\text{m}$  aluminum particles in air. This technique generated a molten particle by melting the tip of an aluminum wire electrode and the initial droplet temperature was a controllable parameter. The initial state of particles produced in this manner did not experience encapsulation by a previously formed oxide barrier coating. This work identified 3 combustion stages: (1) Spherically symmetric vapor phase combustion typical of conventional metal combustion and occurring in a temperature range from 2400  $^\circ\text{C}$  to around 2800  $^\circ\text{C}$ , i.e., near aluminum normal boiling temperature; (2) During the second stage smoke increased and moved closer to the particle surface, the combustion becomes asymmetric and particle spinning is noted; the temperature is found to drop only slightly from the first stage; (3) In the third stage, the particle continues spinning and burning asymmetrically and an oxide cap forms and grows. The particle temperature drops and combustion terminates "when the oxygen content of the molten aluminum droplet reaches the limit needed for alumina formation ( $\sim 14\%$ ) and droplet temperature attains the three phase (liquid AIO solution, liquid  $\text{Al}_2\text{O}_3$  and gas) equilibrium point at 2240  $^\circ\text{C}$ . Rapid changes in the burning particle trajectories observed during the third stage of the combustion are explained by the asymmetric growth of oxide caps on spinning particles". Additionally, an electric field was found to reduce combustion time and affect particle temperature.

In reference [12], Dreizin noted that burning aluminum particles will quench when the particle temperature cools to the  $\text{Al}_2\text{O}_3$  melting point. In this work, Dreizin goes on to refine the temperature range corresponding to the first combustion stage identified in earlier work. The temperature "lies between the boiling points of Al (2520  $^\circ\text{C}$ ) and the melting point of  $\text{Al}_2\text{O}_3$ ".

In reference [13], the ignition model is refined to include a fourth combustion stage and the various solid phases for alumina are related to combustion stages. Further, reaction

kinetics data is provided for the various oxidation stages, as well as the oxide thickness corresponding to 10–14  $\mu\text{m}$  particles subject to a heating rate of 40 K/min. From his model, an oxide thickness of around 70 nm is predicted when the particle is heated to a temperature of 1350 K. For this size particle, the minimum ignition temperature, in air, is predicted to be 2100 K.

In reference [14], aluminum particles in the one  $\mu\text{m}$  size range were ignited by laser in various gaseous environments. The particles were moved across the fixed laser beam at various velocities; the laser beam exposure time was related to the amount of energy imparted to the particle. Then, the minimum laser power to achieve ignition was plotted versus particle velocity for each gas. Gases considered included air,  $\text{CO}_2$ ,  $\text{H}_2\text{O}/\text{N}_2$ ,  $\text{CO}_2/\text{O}_2$  and  $\text{H}_2\text{O}/\text{N}_2/\text{O}_2$ . The finding was that ignition in water vapor was difficult, i.e., required higher threshold energy than the other gas combinations, but when ignition was established, the rate of reaction was higher than in other environments. This work additionally presents global reaction kinetics for each gas based on the Arrhenius model.

Yuasa et al. [15] studied ignition of a solid cylinder of aluminum inductively heated in a flowing oxidizing stream (essentially air composition) over a range of pressures and velocities, and examined the influence of an original oxide coating on the ignition criteria. Without the oxide coating, (actually the original sample had a thin oxide coating which was broken by heating to 1000 °C in argon) the spontaneous ignition temperatures were lower than the melting point of  $\text{Al}_2\text{O}_3$ , and decreased with reduction in pressure and velocity of the gas flow. When an original oxide coating existed on the aluminum, ignition occurred in the gas phase at the instant of the breaking of the coating. For the case with a compromised oxide coating, at an aluminum temperature above 1400 °C, aluminum vapor moving away from the solid surface condensed to form a white smoke. When the oxidizing stream was introduced, the white smoke abruptly stopped and when ignition occurred, the gas phase near the sample surface started to emit light uniformly. Gas phase emission in Al lines and AlO lines became stronger leading to combustion with a fully developed flame. It was found that throughout this process, no reaction film was formed on the surface. On the other hand, in the case of non-ignition, although emission near the sample surface became temporarily stronger just after exposure to the oxidizing stream, the sample surface was immediately covered with an oxide film and emission vanished, suggesting that the oxide film inhibited further oxidation. The ignition temperature for this case was found to be much lower than the melting point of  $\text{Al}_2\text{O}_3$ . For the case of an oxide coated specimen, the coating thickness increased during heating in an oxidizing atmosphere until the coating began to break. As heating continued, the breakage increased until emission in the gas phase was noted and the metallic surface of aluminum was observed and a stable diffusion flame of aluminum vapor was established. For the latter case with a growing oxide coating, the heating rate correlated inversely with ignition temperature (by as much as 400 °C) because slow heating allowed for an increased oxide coating thickness which inhibited the addition of aluminum vapor to the oxidizer.

In later work with the same apparatus [16], the oxygen content of the oxidizing gas was varied and the sample temperature and flame structure during combustion were measured. Their study found: (1) ignition temperature is almost constant irrespective of the oxygen concentration when the sample was heated at constant rate, (2) with increased oxygen concentration, the Al and AlO emission shifted to the aluminum surface in the flame zone, and (3) the burning rate depended on the sample temperature but only slightly on the oxygen concentration. This work also confirmed that first ignition occurs in the region of the cracked oxide coating. Regarding finding 2, as combustion progressed, the temperature of the aluminum sample increased slightly, and the flame zone moved away from the aluminum surface. The higher the oxygen concentration, the faster this occurred. These observations led to the conclusion that as the aluminum vaporization rate increases, the location where the aluminum concentration drops to the rich flammability limit moves farther from the vaporizing surface.

Huang et al. [17] developed a theoretical model in an attempt to rationalize various experimental findings, and compiled data correlating ignition temperature to particle size. For larger particle sizes, e.g., greater than 100  $\mu\text{m}$ , the ignition temperature is near the melting temperature of alumina (2350 K). The oxide shell is weakened near this temperature so that mechanical stresses, such as thermal expansion of the aluminum, can lead to rupture and subsequent ignition. However, for smaller particle sizes, e.g., in the 10  $\mu\text{m}$  range, the ignition temperature is found to be near 1700 K and can drop to around 1000 K for particles in the 0.1  $\mu\text{m}$  range. This work presents a kinetics model for 12 reactions which are assumed to be necessary for the oxidation of aluminum to alumina, including reaction order as a parameter.

Meinkohn [18] examined metal particle ignition in light of the Frank-Kamenetzki theory and differentiates between global and local ignition; the former corresponding to a uniform oxide layer, and the latter corresponding to punctures or ruptures in the oxide coating. With global ignition, threshold is related to loss of stability of the oxide layer, e.g., in order to be stationary requires oxide vaporization to exactly balance solid oxide growth. This, in turn, is related to the oxide flux arriving at the inner surface of the oxide layer. On the other hand, local ignition is by way of oxide layer defects which spread from regions of high permeability to regions of low permeability and ignition is dependent of whether the oxide layer retracts to expose the underlying metal to the oxidizing atmosphere, or whether the oxide layer reforms. For metal combustion, it is local ignition which is at play, so behavior of the local ruptures in the oxide layer region of interest. Important parameters which influence this outcome include particle size, ambient temperature, the oxidizer concentration and the Marangoni number for the oxide. This latter parameter is the temperature sensitivity of the surface tension taken at the constant stationarity condition introduced above, e.g.,  $Ma \sim (\partial\sigma/\partial T)_{(z=h)}$  which at the point of transition from assisted ignition to auto-ignition, changes signs. Meinkohn makes the conclusion that by reducing the oxidizer concentration, the range of conditions under which the oxide layer breaks can be greatly extended.

Bui et al. [19] have made high speed videos of aluminum particles heating on a burning propellant surface and lofting into the gas jet moving away from the surface. This observation is in substantial agreement with Price. An image is shown in Figure 1 illustrating burning surface of ammonium perchlorate propellant with incandescent aluminum agglomerates lofting from the surface.



**Figure 1.** Burning surface of ammonium perchlorate propellant with incandescent aluminum agglomerates lofting from the surface.

The comet tail ahead of the particles is presumably alumina smoke from gas phase oxidation of the aluminum which is carried forward of the particle by gases emanating from the propellant surface.

It has been speculated that melted aluminum particles in pockets beneath the burning propellant surface are undergoing agglomeration and grow from nominal 30  $\mu\text{m}$  to several times that diameter. In this work, combustion test results are presented along with research

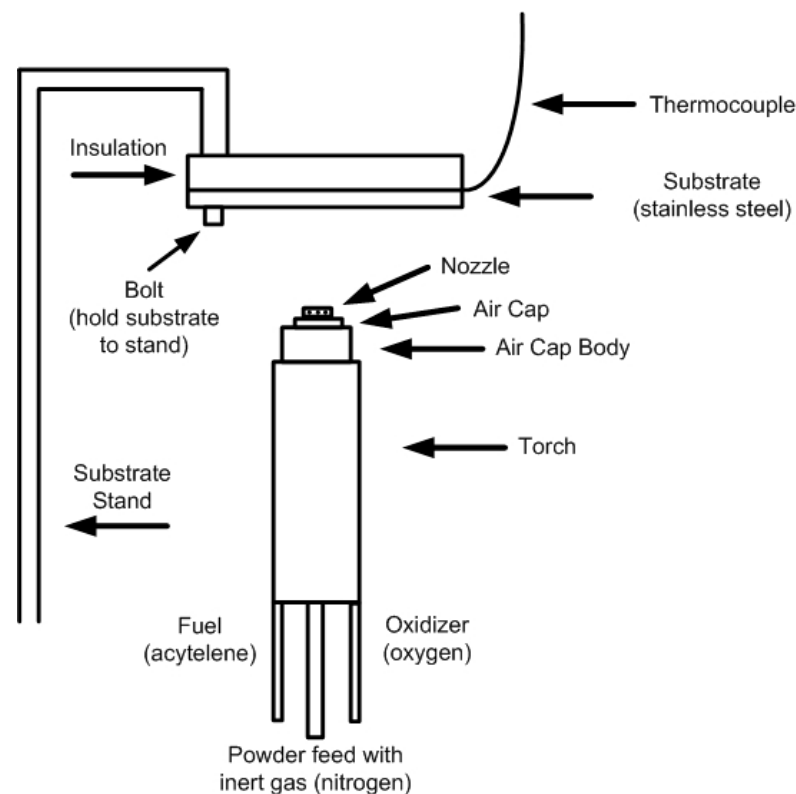
in which the heat source and rate of heating of aluminum were varied. It is noted that while the volume of work reported in the literature is enormous, the present objective is to focus on atmospheric pressure combustion behavior, and in particular, those studies where the influence of the oxide layer is addressed.

## 2. Experimental Work and Results

The following sections provide details about experiments and results involving oxyacetylene torch, thermogravimetric analysis with differential scanning calorimeter, aluminum particle heating, electric ignition and aluminum powder heating.

### 2.1. Oxyacetylene Torch Experiments

Experiments utilized an oxyacetylene torch with a powder feed capability to simulate a small propellant fire. The combined combustion gases and injected aluminum particles then impacted a target stainless steel plate located approximately 1.5"–6" (3.81–15.24 cm) from the torch tip. The plate was equipped with an intrinsic type K thermocouple affixed to the backside for estimation of heat flux attendant to the aluminum powder. The plate was insulated on the back surface and would typically be preheated by the torch to order of 1000 °C before the powder feed was started. Figure 2 illustrates the experiment set-up. The torch is capable of various configurations for adjustment of flame temperature, particle temperature and particle velocity.



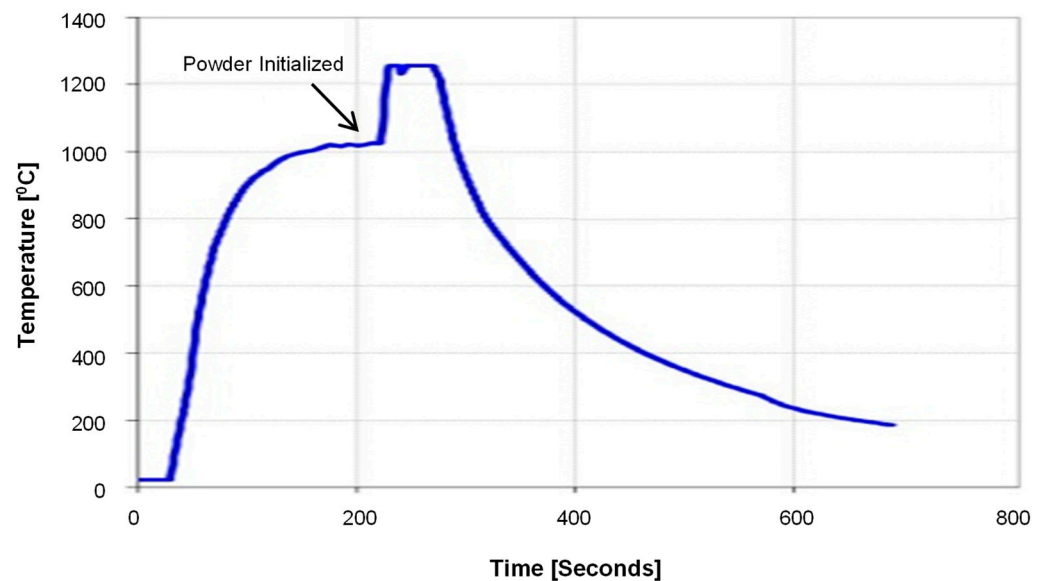
**Figure 2.** Schematic diagram of the experimental apparatus showing torch and target plate.

Figure 3 illustrates post-test of target showing unburned aluminum deposits near center of torch jet projection. (white deposit appears to be alumina smoke, and surrounding black is soot from acetylene during ignition.)



**Figure 3.** Post-test of the plate.

Figure 4 shows temperature measurement on back side of a stainless steel plate preheated by gases from the oxyacetylene torch, followed by injection of 30- $\mu\text{m}$  aluminum powder. For this measurement, distance from torch tip to calorimeter is 3 inches (7.62 cm). Powder feed was performed at 700 rpm. Thermocouple reading was approximately 1020 °C before power was initialized. The upper temperature plateau represents limit in algorithm for converting thermocouple voltage to temperature.



**Figure 4.** Temperature measurement on back side of a stainless steel plate preheated by gases from the oxyacetylene torch, followed by injection of aluminum powder.

Figures 5 and 6 show SEM and EDS images of the surface deposit on the stainless steel target. SEM image in Figure 6 reflects a small portion of what is shown in Figure 5. Point 1 shows composition in stainless steel area (white region in the SEM image). Point 2 shows composition in inter-metallic zone. Point 3 shows composition of aluminum zone.

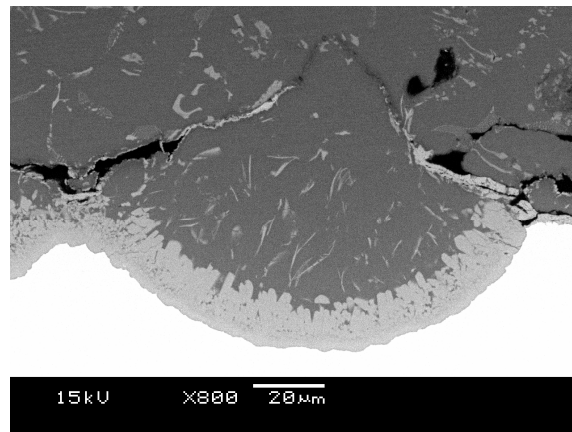


Figure 5. Polished section of the affected zone on the stainless steel plate (bottom white is stainless steel).

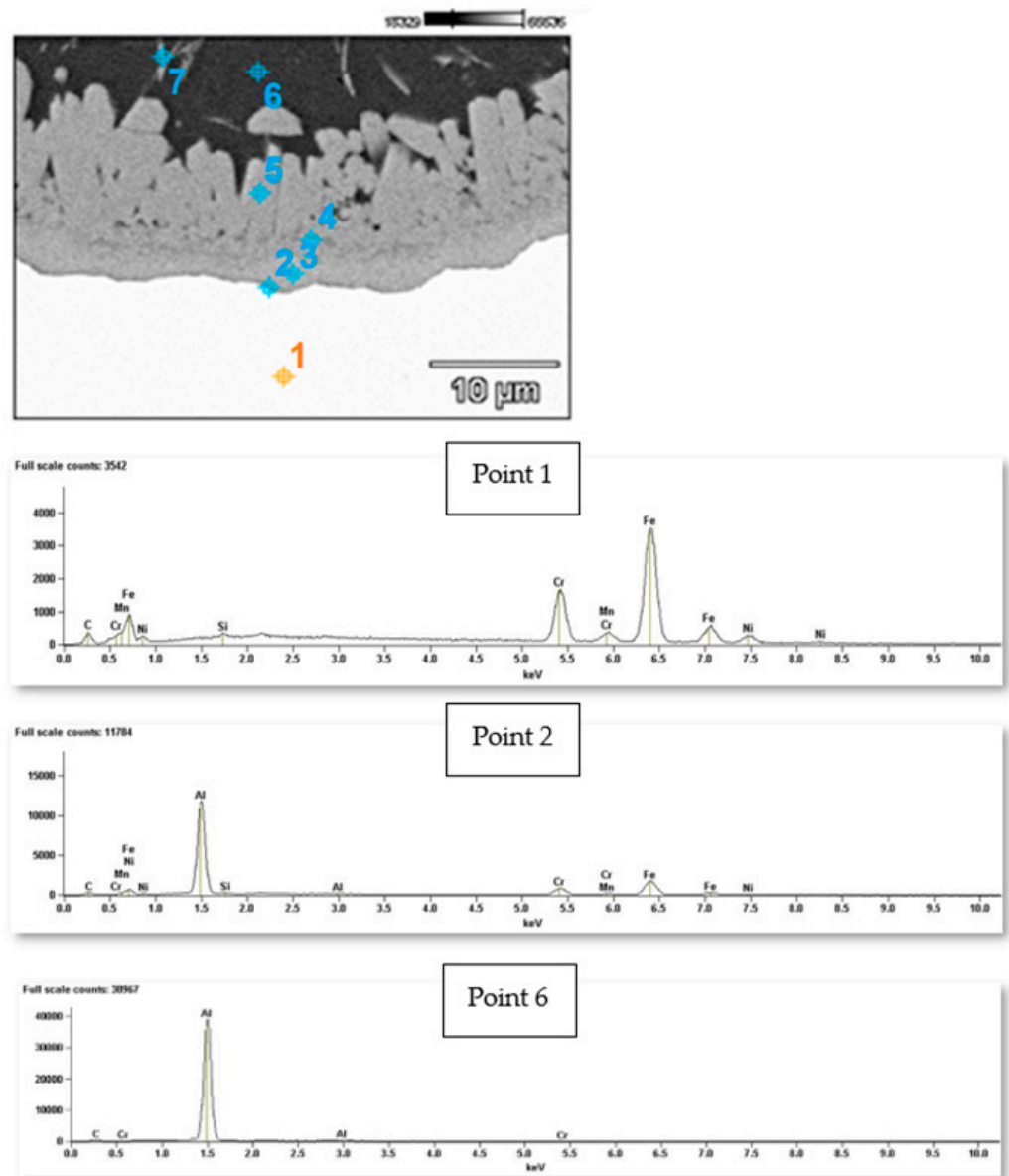
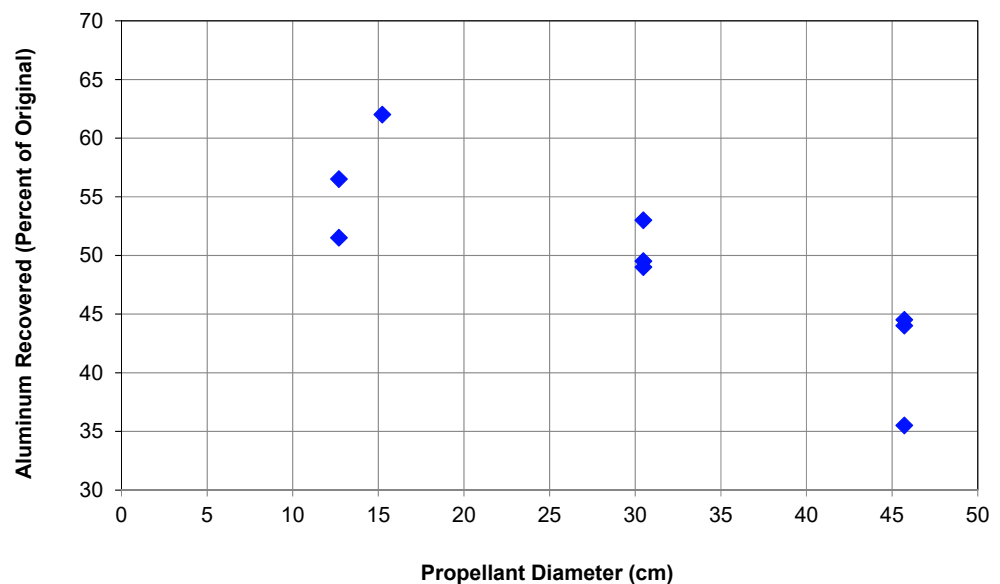


Figure 6. EDS composition estimates.

SEM and EDS illustrate that the aluminum powder was not oxidized by the torch at conditions of this test, even though the adiabatic temperature of an oxyacetylene torch is on order of 3500 °C. However, thermocouple data from the series of tests show that a significant increase in target temperature occurs when aluminum powder is introduced to the flame. This is presumably due to the enhanced heat transfer as droplets of liquid aluminum collect on the target surface and freeze, thus releasing their enthalpy of fusion.

Additionally, experiments involved large scale gravimetric analysis of deposits which were swept from the floor following actual downward burns of an aluminized composite propellant with a gap between the propellant and a graphite target plate and compared this result to the original aluminum content of each propellant charge which was tested. The assumption is that the fraction of aluminum powder originally in the propellant which was oxidized to alumina passed up the vent of the burn chamber and was not collected on the floor. So the collected residue should essentially reflect the unburned fraction. Figure 7 shows fraction of collected residue after various diameter propellant charges were burned.



**Figure 7.** Fraction of original aluminum content of propellant charge which remains as residue after the burn.

It can be observed that as the size of the propellant charge increases, the fraction of free aluminum decreases. This observation appears to indicate that the higher interior temperature of a large burn results in a higher fraction of aluminum oxidation.

Similar results were obtained for upward burns using coupons inserted into a burning propellant plumes for 5 s. Later, the deposit was analyzed to determine the degree of oxidation of aluminum which was scraped from each coupon. The extent of oxidation was determined by using a differential scanning calorimeter (DSC) to determine melt energy when the sample was heated to temperatures above the melting point of aluminum, and comparing this amount of energy to the mass of the sample. Results are shown by Figure 8. This plot indicates that aluminum continues to oxidize in the plume up to at least 30 inches (76.2 cm) above the propellant surface and that the ratio of unreacted aluminum to original aluminum in the propellant decreases with increasing charge diameter, at least at heights above 10" (25.4 cm). Temperature measurements as a function of height in upward propellant burn as well as extensive validation studies are reported in the literature [2,20].

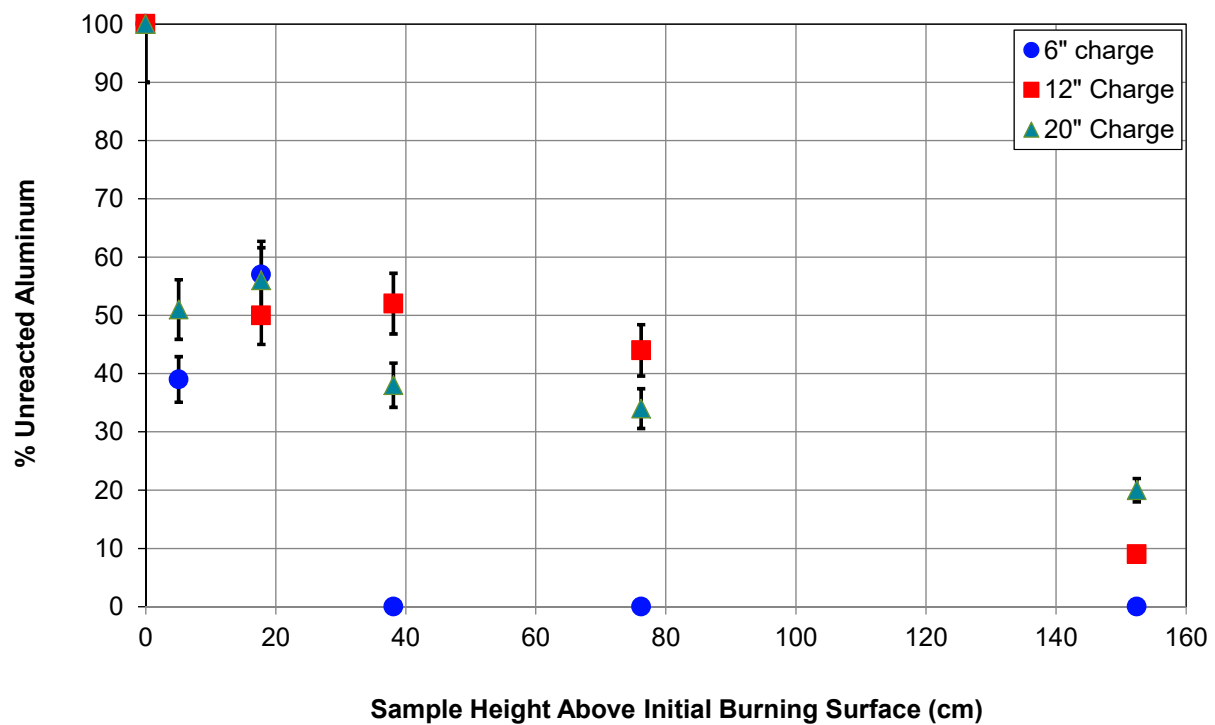


**Figure 8.** Fraction of unreacted aluminum from deposit on coupons inserted into a propellant plume.

## 2.2. Thermogravimetric Analysis with Differential Scanning Calorimeter

Thermogravimetric Analysis with Differential Scanning Calorimeter (TGA-DSC) was used to measure weight gain and heat flow in the presence of an oxidizer as a sample is heated. This measurement was performed on nominal 10  $\mu\text{m}$  aluminum powder. Previous attempts indicated that when the particles are heated in the presence of an oxidizer, an oxide shell forms which is sufficiently thick that full combustion is not observed up to the limit of the apparatus (up to 1600  $^{\circ}\text{C}$ ). Subsequent tests utilized heating of aluminum to test temperature in argon, and then oxygen was introduced. Heating in argon does not grow the initial oxide shell so that when oxygen is introduced combustion can be experienced at much lower temperatures than the alumina melting temperature. This is an excellent technique to visualize the effect that an oxide shell has on the combustion of aluminum.

Figure 9 shows the results for a test in which a temperature of 1400–1450  $^{\circ}\text{C}$  was reached before introduction of oxygen. In this figure, when the oxidizer was introduced, an exothermic reaction occurred. This resulted in a rapid temperature rise, along with increasing mass which signified oxygen uptake. Performing a simple mole balance of the mass increase in Figure 9 (right side shows ratio of the aluminum to oxygen is approximately 0.82 on a mole basis; for complete combustion, a ratio of 0.67 is needed. Hence, the oxidation was not quite complete. The results of this study show the effect that an alumina shell has on the particle combustion temperature. Further investigation of heating an aluminum particle should be conducted in order to determine the lowest temperature for ignition. However, it is likely that the submicron particles which are attached to the nominal 10  $\mu\text{m}$  particles are responsible for the lower ignition temperature which subsequently ignited almost all of the samples.

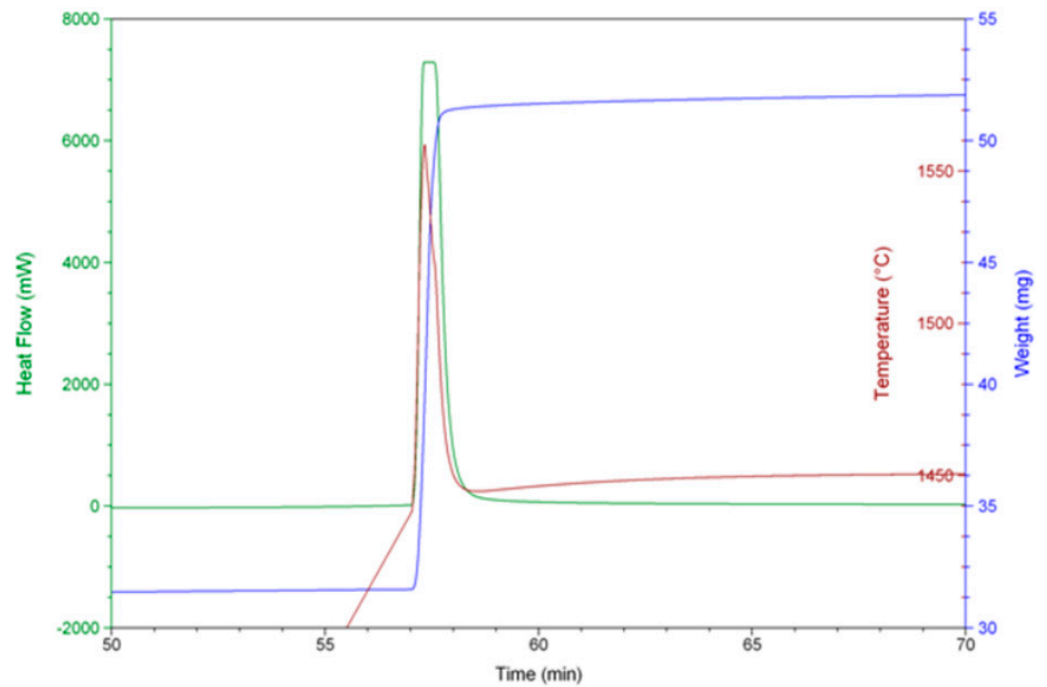


Figure 9. Temperature of 1400–1450 °C was reached before oxidizer was introduced.

Tests were performed on aluminized composite propellant. The residual powder that was swept from the test site was encapsulated, and then polished to yield an inside look at some of the aluminum particles. Figure 10 shows SEM image of particle cross-sections from residue following propellant test. Image is much larger than original aluminum particles, perhaps showing evidence of agglomeration, and contains interior aluminum core. Figure 11 provides EDS of the particle shown in Figure 10.

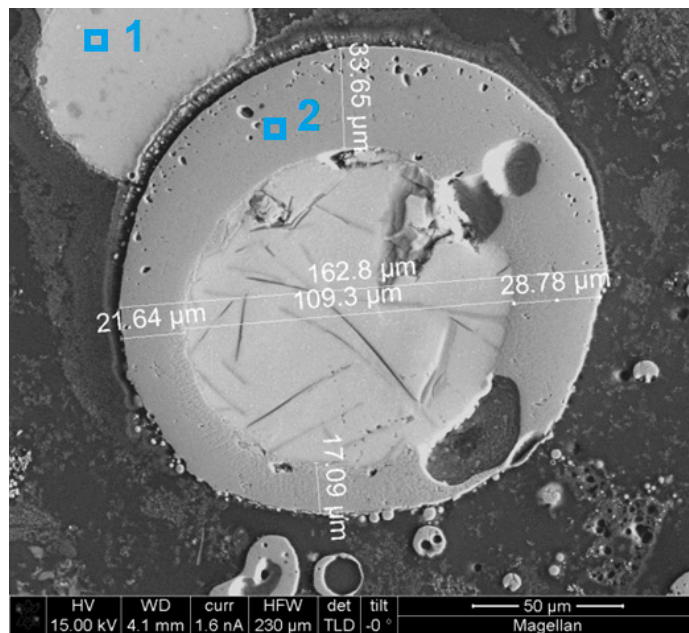


Figure 10. SEM image of particle cross-sections from residue following propellant test.

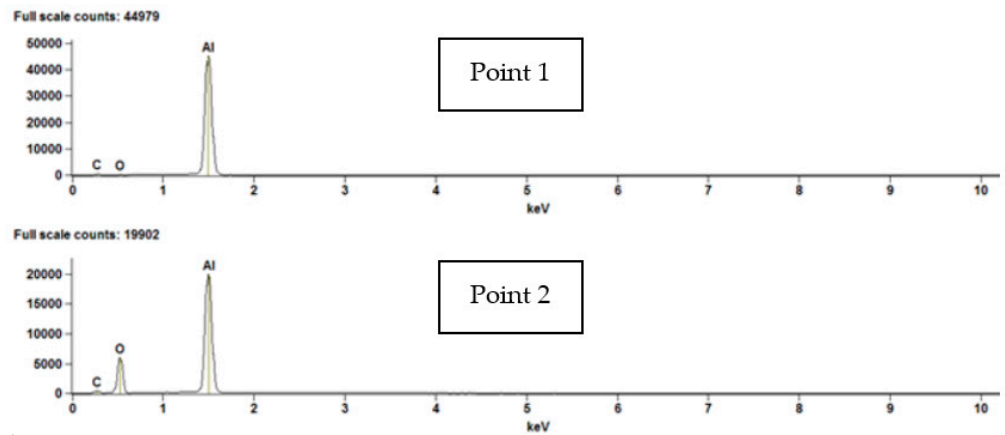


Figure 11. EDS of particle shown in Figure 10.

An alumina shell about 25  $\mu\text{m}$  thick encompasses the agglomerated aluminum particle but for the particle shown in Figure 12, agglomeration was not evident and the center of the particle is a void.

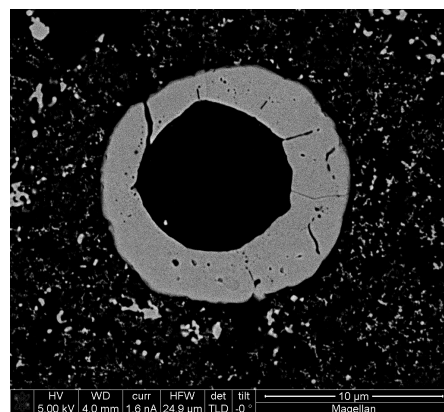


Figure 12. Empty oxide shell collected on chamber floor following burn.

However, for other particles, an alumina cap was observed on the surface, similar to that seen by Price et al., and is shown in Figure 13. The size of this particle is presumably the result of agglomeration of smaller aluminum particles which were originally formulated with the propellant. Note that this particle is significantly larger than nominal 30  $\mu\text{m}$  powder which was presumably used in the propellant formulation.

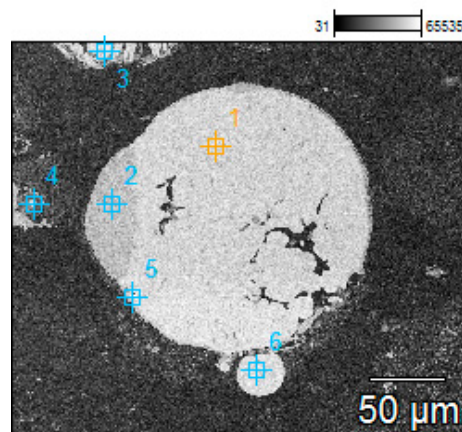


Figure 13. Oxide cap and thin surface oxidation.

According to the EDS results shown in Figure 14, point 1 of Figure 13 consists of almost pure aluminum and point 2 contains species/mixture of aluminum with some oxide. In Figure 15, the green cap and shell around particle indicates oxygen presence, whereas light blue shows only aluminum but a dark blue indicates aluminum presence along with oxygen in the cap and shell. Since these tests were performed at atmospheric conditions it can be presumed that exposure to atmospheric oxygen was responsible for the thin aluminum oxide layer appearing around the outer surface of the particle. The EDS of the residue does confirm that the majority of the solid was indeed raw aluminum and the amount of oxygen indicated was consistent with a surface oxide.

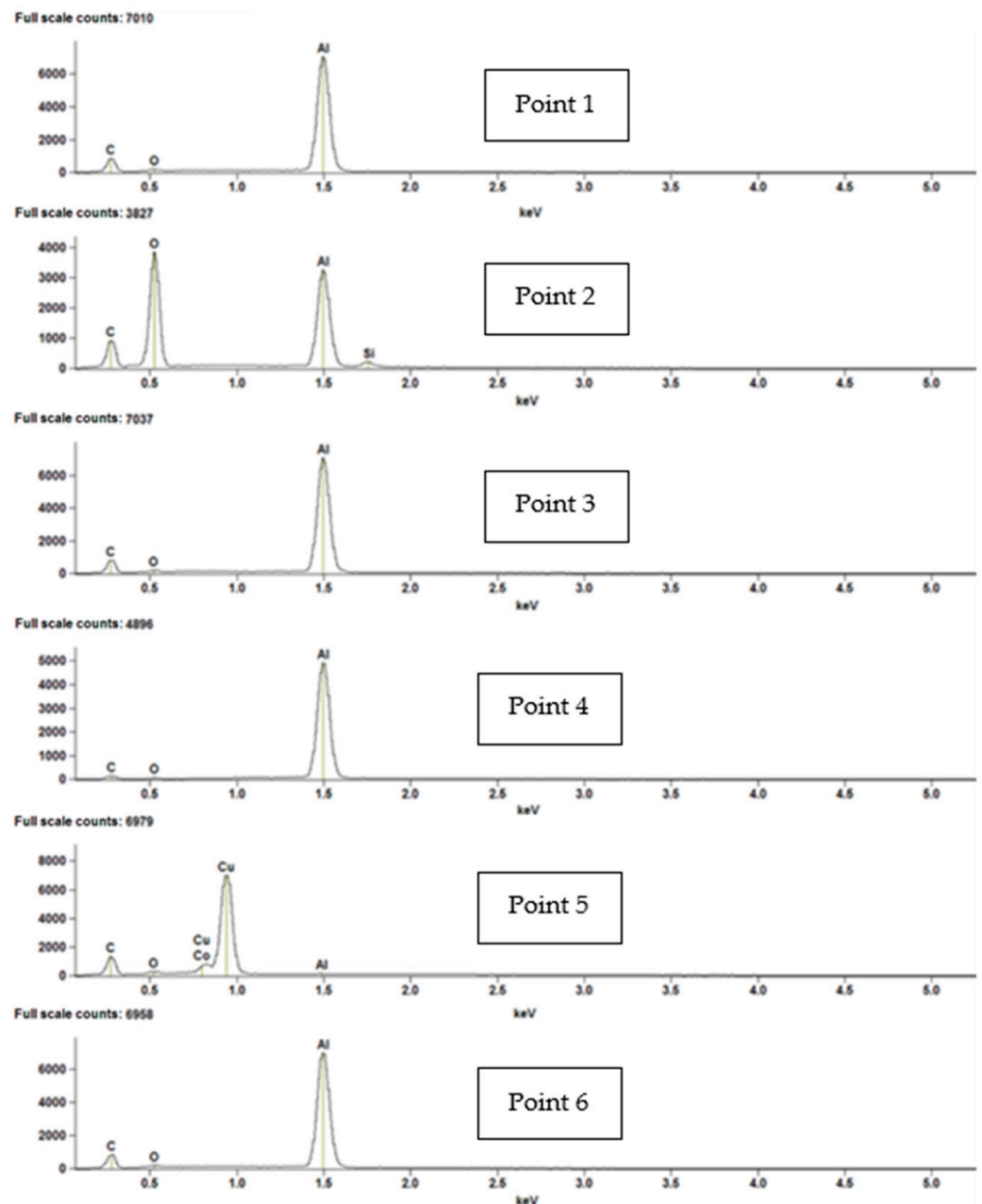
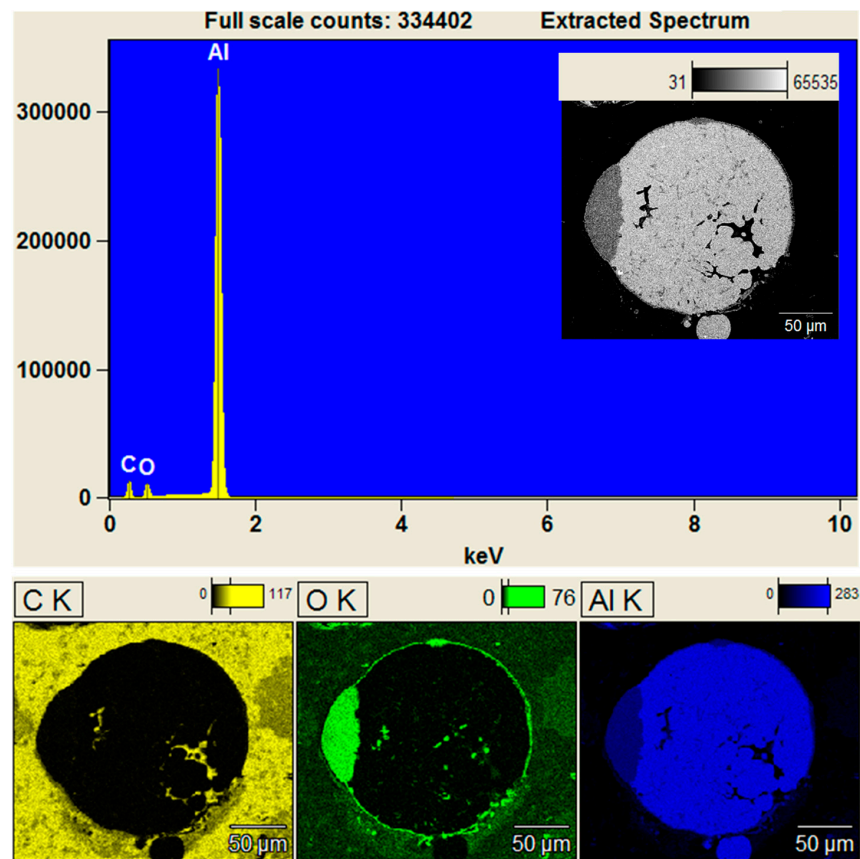


Figure 14. EDS of an aluminum particle with agglomerate.



**Figure 15.** Demonstration of SEM/EDS data to illustrate oxide cap and surface oxidation on aluminum particle.

Figure 16 is a photograph taken during the burning of a 5" (12.7 cm) diameter charge of aluminized composite propellant. Near the base of the charge, some white streamers plunging downward can be observed. These are presumably aluminum particles which are burning and emitting a smoke trail of  $\text{Al}_2\text{O}_3$ . On the other hand, some luminous particles can be observed near the top of the burning zone which are not associated with smoke production. It may be that these are agglomerated aluminum particles which have formed a protective oxide barrier and are not still burning at this location. The blacked out band is a sensor array located closer to the plume.



**Figure 16.** This is an image from a burning 5" (12.7 cm) diameter charge of aluminized composite propellant.

### 2.3. Aluminum Particle Heating

Aluminum particles were heated utilizing a MIG (metal inert gas) welder with aluminum wire feed. The following Figures 17–19 show that ignition can be accomplished by this method, and the apparent outcome of the particle striking a stainless steel plate is governed by the current setting on the welder, i.e., initial energy state is controllable. Figure 20 shows aluminum un-oxidized particles which were either not ignited, or ignited and quenched on stainless steel plate after MIG heating. These observations show the effect of particle size, temperature and velocity on particle-wall interaction. Due to a number of factors, particles may adhere, rebound, spread, break-up and rebound, break-up and spread, or splash [1].



**Figure 17.** Un-ignited aluminum particles sticking on impact with SS plate.



**Figure 18.** Ignited aluminum particles (based on white smoke following particles) rebounding following impact on a SS plate and not quenching.



**Figure 19.** Apparent fragmentation of ignited aluminum particles on impact with SS plate.

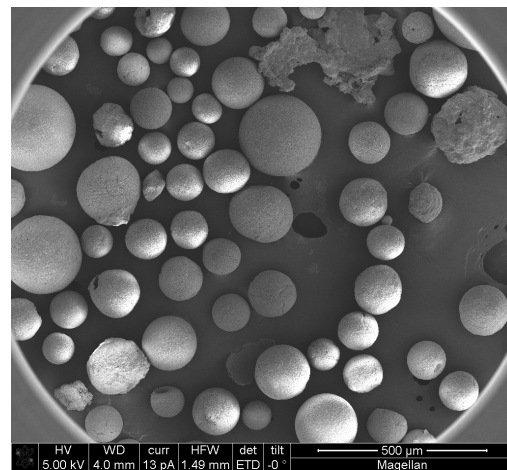


**Figure 20.** Aluminum un-oxidized particles collected after MIG heating and either not ignited, or ignited and quenched on stainless steel plate.

#### 2.4. Electric Ignition

Attempts at electrical ignition were performed using capacitor discharge current through a fine aluminum wire which had been intentionally pre-oxidized by mild resistive heating in the same fixture as used for ignition. The purpose of this approach was to avoid repositioning of the wire between conditioning and ignition testing. The approach suffered from two shortcomings. First, since the wire was not high purity but included silica as point occlusions, this caused localized concentration of the electrical current and overheating at that location. This in turn, led to local evaporation of the underlying aluminum which vented through ruptures in the oxide layer but did not ignite. Then, on capacitor discharge heating of the wire, failure or ignition occurred preferentially in these point-compromised regions. Secondly, the posts to which the wire was attached were fixed, so that expansion of the wire caused stress breaks in the oxide layer and provided an unintended preferential point of ignition. Figure 21 illustrates a point where localized heating occurred during the oxidation growth stage and shows evidence of internal aluminum melting and material ejection [21].

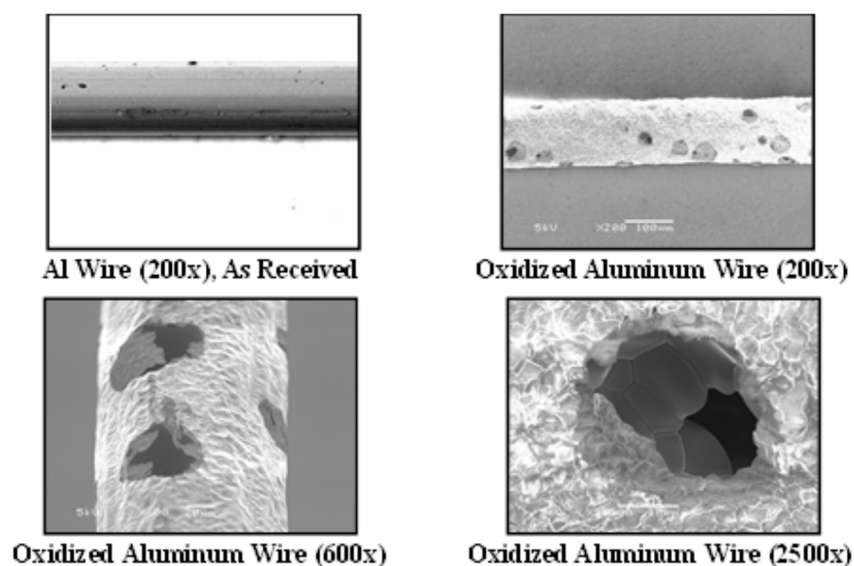


**Figure 21.** Illustration of damage due to localized heating apparently caused by silica inclusions in the wire.

Figure 22 shows stress deformation of the wire when a capacitor was discharged through the wire, not resulting in ignition. This result shows that failure points in the oxide coating provide the pathway for aluminum vapor to escape and mix with ambient air, and potentially result in ignition if conditions are sufficient, e.g., energy state sufficiently elevated, and the mixture is within the flammability limits for aluminum vapor and air. It was an observation that if ignition did occur, as evidenced by emission of radiation passing through a narrow band pass filter of 480–490 nm wavelength (AlO emission), the point of ignition did not occur at the midpoint of the wire, but rather near the clamps where bending stress in a buckling column (from thermal expansion of the wire between fixed posts) would be high. Figure 23 shows evidence of “healing” of breaches by new oxide growth.

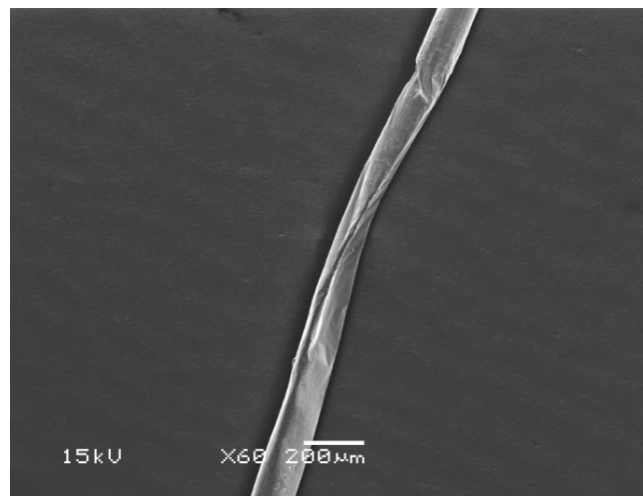


**Figure 22.** Evidence of wire stress caused by capacitor discharge through wire (note, wire did not ignite).

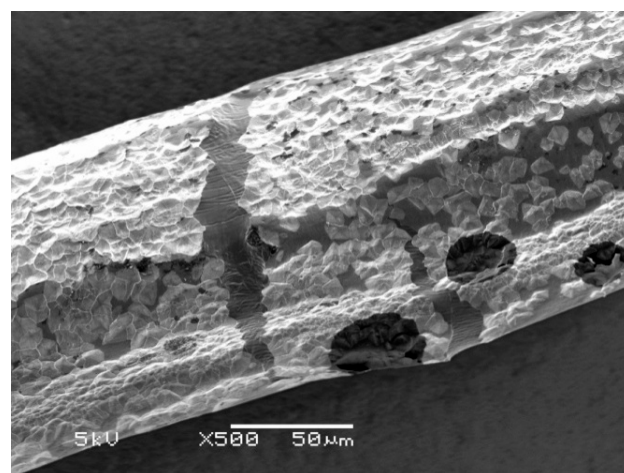


**Figure 23.** Evidence of healed of breaches in the oxide layer.

### 2.5. Aluminum Powder Heating

Two different apparatus were constructed for heating 10 µm, nominally sized, aluminum powder. The dimensions and size distribution can be seen in Figure 24. It is important to note that although this powder sample is nominally 10 µm, there are some particles much smaller, on the order of 1 µm or less. When the samples are sieved, it is apparent that the smaller particles remain attached to larger particles. According to Huang [17], these smaller particles can ignite at much lower temperatures than the melting point of alumina, and may play a role in promoting at least partial ignition.

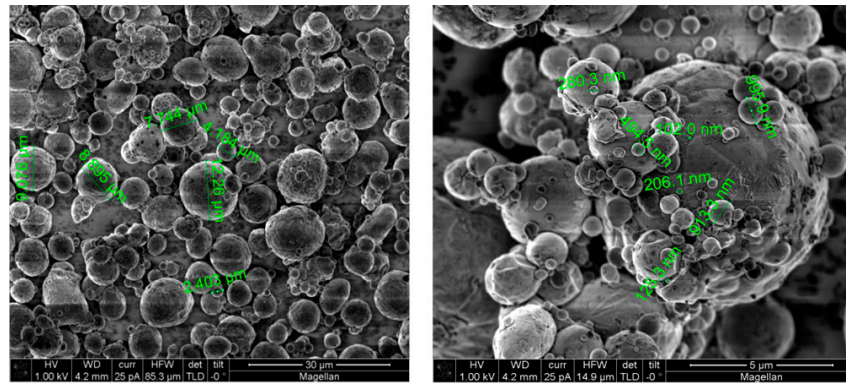


**Figure 24.** Two SEM images showing size distribution; 10 µm nominal aluminum powder specified.

In the first apparatus, aluminum was dropped onto an electrically heated Ni-chrome foil strip. Figure 25 below shows a series of six images from a typical test.

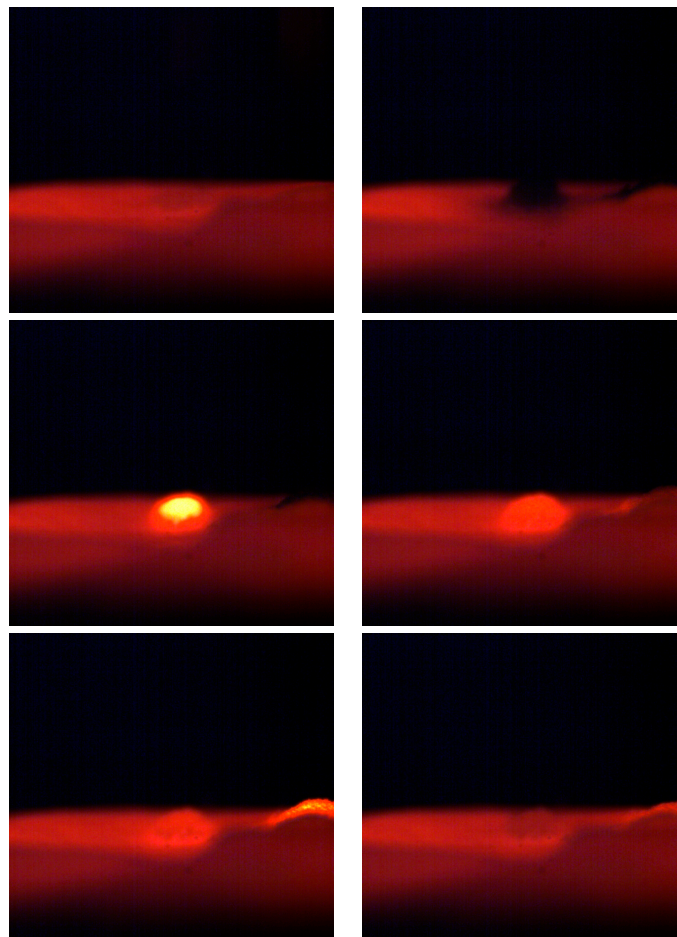


**Figure 25.** Ignition sequence (left to right, top to bottom) for 10 µm Al powder falling onto Ni-chrome ribbon at approximately 1200 °C. The total time from falling on the foil until achieving equilibrium with the foil is about 0.04 s.

As the frames progress, an aluminum particle or cluster falls onto the hot surface, absorbs energy by melting and then begins to emit light as it ignites. So: (1) the top left frame shows the hot foil before particles fall onto it; (2) the top right frame shows a dark region where heat is being absorbed from the foil as the aluminum particles melt, (3) the middle left frame shows the incandescence, indicating some sort of ignition, (4) the middle

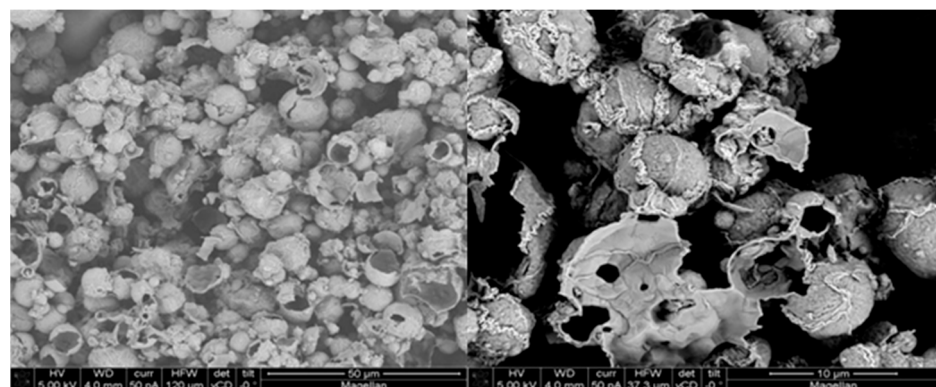
frame right shows the initial site cooling, while at the same time, some particles fall onto a location to the right, (5) on the bottom left frame, the initial site is no longer incandescent but the second location is emitting, and (6) in the last frame bottom right, both locations are shown to cool. A crust which is presumably alumina retains some shape since it does not melt and merge with the hot foil.

Figure 26 shows a magnified view of an ignition region where the ignition appears to cause a local “eruption” with strong emission in the visible wavelengths.



**Figure 26.** Image showing close-up combustion of a cluster of 10  $\mu\text{m}$  aluminum powder dropped on a Ni-chrome ribbon preheated to  $\sim 1300$  °C.

After the particles were seen to have ignited, a SEM image of the residual deposit was taken; these images are shown in Figure 27 (lower magnification on left, higher on right) with EDS of the shell shown in Figure 28. High oxygen/aluminum ratio indicates alumina (non-calibrated intensity). The particle cluster appears to be made up of shells of alumina. This observation agrees with a previous study done by Price et al. [9]. That study states that shell rupture occurs due to fractures caused by cracks, which allows the aluminum to vaporize more rapidly and react with the oxidizing atmosphere. Ignition may or may not have resulted, depending on favorable conditions; in particular, a sufficiently energetic state and the aluminum vapor and oxygen from the air meeting within the flammability limits. In this experiment, ignition and combustion were apparent from observation during the experiment and then confirmed using SEM imaging. These ignition temperatures were well below the melting point of alumina.



**Figure 27.** Two SEM images of aluminum particle clusters heated by dropping onto hot Ni-chrome ribbon.

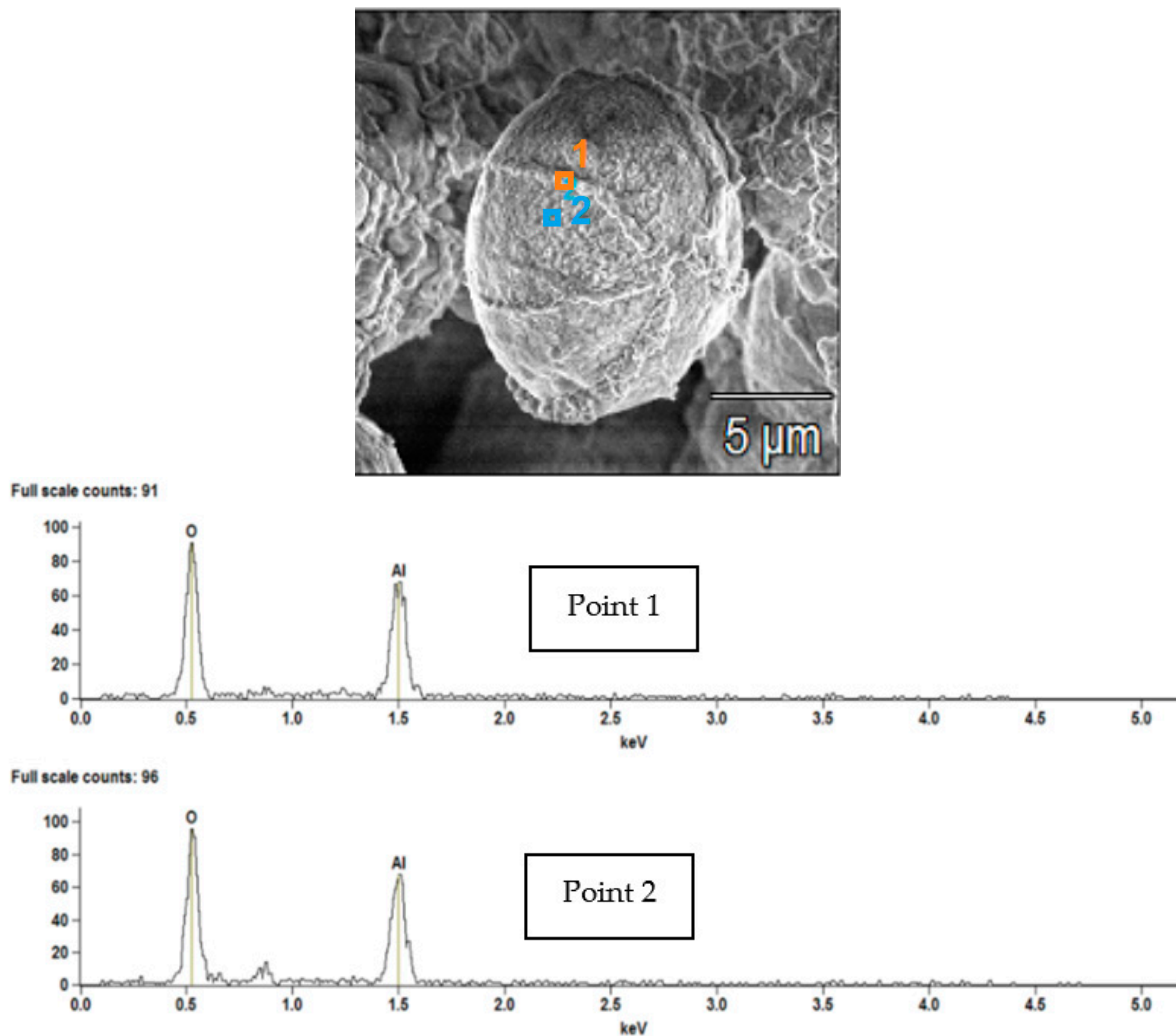


**Figure 28.** SEM and EDS for a particle in a cluster which had been dropped onto a Ni-chrome foil.

The second experiment utilized a graphite resistance heater where aluminum particles were heated to the range 900–1200 °C in increments of 50 °C. The particles were dropped through the 12" long × 2" diameter (30.48 cm × 5.08 cm) graphite heater tube which allowed small clusters of powder to be captured at the bottom of the tube for study. The residue was examined by SEM to determine the state with regard to oxidation and physical appearance. It was noted that for the higher preheat temperatures, white smoke was observed emanating from the heater which may be either alumina smoke, or condensing aluminum vapor. Figures 29 and 30 show SEM and EDS images, respectively, for particles involved in some of the tests. The particles have the appearance of a deflated soccer ball with dimples indicating shrinkage after cooling. Shrinkage could be a consequence of cooling following thermal expansion of the oxide coating, or may be a consequence of aluminum vapor escaping from the particle. Since breaches in the oxide coating are not apparent, this may support the contention that the event was a simple thermal expansion following by cooling contraction.

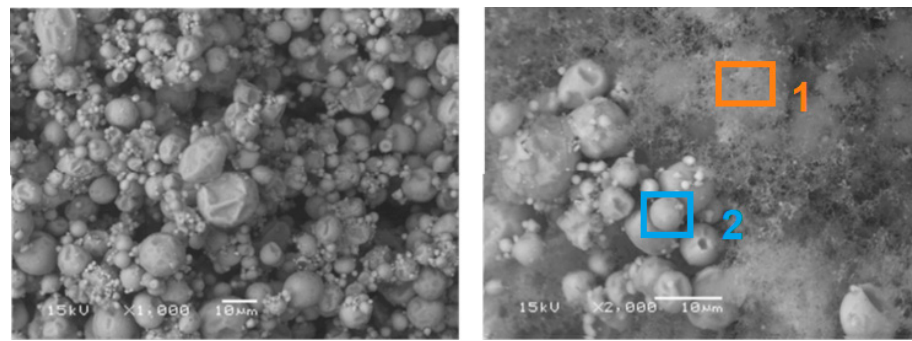


Figure 29. Aluminum particles exposed to 1000 °C (right), 1150 °C (left).

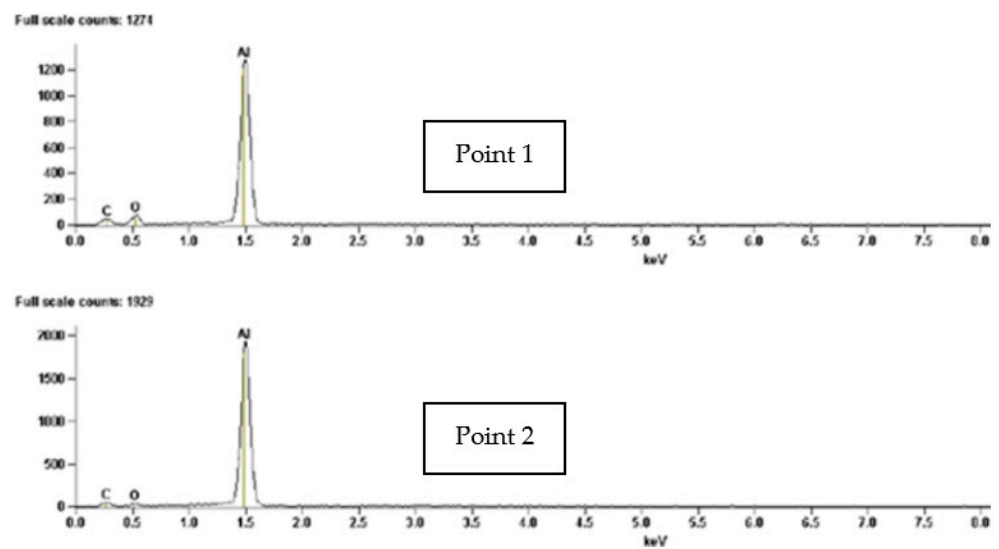


Figure 30. EDS image of right image from Figure 29, showing residual from heated aluminum particles.

Although alumina smoke was observed on the tube of the apparatus, EDS and SEM imagery could not conclude from the particle forensics that ignition occurred. While apparent ignition was at a lower temperature in these tests than much previous work which opined that the melting point of alumina was necessary for ignition, it is apparent from the SEM particle size distribution, that there are copious quantities of submicron particles attached to nominally sized particles. Hence, according to Huang [17], it may be that only these very small particles are igniting early, and not providing sufficient energy to ignite nominally sized particles.

### 3. Discussions

Aluminum behavior when heated has presented a number of unresolved questions which perhaps should be considered in designing future experiments to better understand phenomenology related to solid propellant burning at atmospheric pressure. These follow:

- One of the first questions should consider whether or not heating single aluminum particles in a known gas composition is representative of heating agglomerates on a propellant surface where the gas chemical composition is unique. Chlorine (a major constituent in the propellant plume) can be sampled by EDS but this choice must be included in selection prior to conducting measurement; previous investigation did not make this choice.
- Another question concerns behavior of agglomerate on a burning propellant surface. What is the mechanism of loft into the flowing product gases which jet away from the propellant surface and how does the native particle oxide layer migrate at temperature?

Lofted particles have been observed to spin and form an oxide cap. Is the artificial gravity due to spinning the mechanism for concentrating the less dense alumina on a non-vertical position on the particle? Does the oxide cap initially form at the top of the agglomerate due to buoyancy and block aluminum vaporization except on the bottom which provides for lofting propulsion?

- Based on evidence of a thick oxide shell forming on the agglomerate which may vent interior aluminum vapor to mix with oxidizer and react in the gas phase, what happens to this thick oxide shell in the propellant plume? These particles, while being composed of alumina, just as smoke, they should be distinguishable. These particles may not remain entrained in the gas stream which jets from the burning propellant surface. Sampling at various locations external to the plume may shed light on this question. A series of vertical pans or trays, alongside the plume may provide information.
- The data collected so far confirms ignition phenomena are dependent on ignition power but further work is needed to characterize this dependence.
- Finally, why do some propellant burns appear to produce copious quantities of unreacted aluminum residue, whereas for other tests with the same nominal propellant, very little debris appears on the chamber floor? This issue may simply be addressed by using a burn chamber with unobstructed access to the chamber floor, and sweeping the floor thoroughly after each test for examination of the debris. However, it may be that the history of the aluminum powder, prior to being cast into the propellant, may not be well controlled and hence, confound interpretation of results.

#### 4. Conclusions

In this work, several experiments including oxyacetylene torch tests, thermogravimetric analysis with DSC, aluminum particle heating, electric ignition and aluminum powder heating, were performed to better understand the impact of oxide layer on aluminum particle combustion. Throughout the studies that have been conducted, a majority opinion is that aluminum begins to combust in air once the melting point temperature of aluminum oxide is reached. The belief is that the integrity of the oxide barrier is compromised and aluminum vapor is able to escape and oxidize with inward diffusing air. However, some research has found that a lower temperature can yield ignition of aluminum as well, particularly if the particles are heated very quickly before the oxide layer can grow to a significant thickness, or if heating is first carried out in the absence of oxygen so that the oxide layer does not grow or if the particles are small  $\sim 0.1$  ( $1 \mu\text{m}$ ). It can also be conjectured that flaws or weak points in the oxide shell can provide a premature breach point where the oxide barrier will fail mechanically and allow aluminum vapor to escape at temperatures lower than that required for the oxide coating to reach its melting point.

There is a significant purpose to continue to elucidate the criteria for particle combustion in the ambient atmosphere; along with the effects incurred from an oxide layer to obstruct these reactions. Pursuing this knowledge will help better understand ignition criteria and support model development for projecting the thermal environment to which a payload could be exposed in the event of an accidental launch pad solid propellant fire. Overall, the results presented in this paper are not intended to be definitive, rather they are presented as useful information for consideration in defining further work.

**Author Contributions:** Writing—original draft preparation, N.Y., B.D. and W.G.; writing—review and editing, N.Y., B.D. and W.G. All authors have read and agreed to the published version of the manuscript.

**Funding:** This research received funding from NASA Jet Propulsion Laboratory (JPL).

**Institutional Review Board Statement:** Not applicable.

**Informed Consent Statement:** Not applicable.

**Data Availability Statement:** Not applicable.

**Acknowledgments:** Sandia National Laboratories is a multi-mission laboratory managed and operated by National Energy Solutions, LLC, a wholly owned subsidiary of Honeywell International, Inc. for the U.S. Department of Energy's National Nuclear Security Administration under contract DE-NA-0003525. The views expressed in this article do not necessarily represent the views of the US Department of Energy or the United States Government. The authors would like to acknowledge the participation of many individuals at both Sandia National Laboratories and students at New Mexico State University. And lastly, financial support from NASA JPL is gratefully acknowledged.

**Conflicts of Interest:** The authors declare no conflict of interest.

## References

1. Yilmaz, N. Modeling of aluminum particle ignition behavior in open atmosphere rocket propellant fires. *Proc. Inst. Mech. Eng. Part G J. Aerosp. Eng.* **2016**, *230*, 690–697. [[CrossRef](#)]
2. Griego, C.; Yilmaz, N.; Atmanli, A. Analysis of aluminum particle combustion in a downward burning solid rocket propellant. *Fuel* **2019**, *237*, 405–412. [[CrossRef](#)]
3. Griego, C.; Yilmaz, N.; Atmanli, A. Sensitivity analysis and uncertainty quantification on aluminum particle combustion for an upward burning solid rocket propellant. *Fuel* **2019**, *237*, 1177–1185. [[CrossRef](#)]
4. Yilmaz, N.; Vigil, F.M.; Tolendino, G.; Gill, W.; Donaldson, A.B. Effect of oxide layer formation on deformation of aluminum alloys under fire conditions. *Proc. Inst. Mech. Eng. Part L J. Mater. Des. Appl.* **2016**, *230*, 879–887. [[CrossRef](#)]
5. Yilmaz, N.; Vigil, F.M.; Vigil, M.S.; Branam, R.; Tolendino, G.; Gill, W.; Donaldson, A.B. Effect of grain orientation on aluminum relocation at incipient melt conditions. *Mech. Mater.* **2015**, *88*, 44–49. [[CrossRef](#)]
6. Lee, D.O.; Hardee, H.C.; Donaldson, A.B. *Thermal Model for Solid Propellant Fires*; SAND75-0051; Sandia National Laboratories: Albuquerque, NM, USA, 1975.
7. Friedman, R.; Macek, A. Ignition and Combustion of Aluminum Particles in Hot Ambient Gases. *Combust. Flame* **1962**, *6*, 9–19. [[CrossRef](#)]
8. Gal'chenko, Y.A.; Gringor'ev, Y.M.; Merzhanov, A.G. Ignition of Aluminum in Carbon Dioxide. *Combust. Explos. Shock. Waves* **1973**, *9*, 115–119. [[CrossRef](#)]
9. Price, E.W.; Sigman, R.K.; Sambamurthi, J.K.; Park, C.J. *Behavior of Aluminum in Solid Propellant Combustion*; DTIC ADA118128; Air Force Office of Scientific Research: Arlington VA, USA, 1982.
10. Bucher, P.; Yetter, R.A.; Dryer, F.L.; Parr, T.P.; Hanson-Parr, D.M.; Viceni, E.P. Flame Structure Measurement of Single, Isolated Aluminum Particles Burning in Air. *Combust. Inst. Symp. Int. Combust.* **1996**, *26*, 1899–1908. [[CrossRef](#)]
11. Dreizin, E.L. *Stages in AL Particle Combustion in Air*; NASA-CR-202812; AeroChem Research Laboratories: Princeton, NJ, USA, 1994.
12. Dreizin, E.L. Experimental Study of Stages in Aluminum Particle Combustion in Air. *Combust. Flame* **1996**, *105*, 541–556. [[CrossRef](#)]
13. Trunov, M.A.; Schoenitz, M.; Dreizin, E.L. Effect of polymorphic phase transformations in alumina layer on ignition of aluminum particles. *Combust. Theory Model.* **2006**, *10*, 602–623. [[CrossRef](#)]
14. Mohan, S.; Dreizin, E.L. Aluminum particle ignition in mixed environments. In Proceedings of the 47th AIAA Aerospace Sciences Meeting, Orlando, FL, USA, 5–8 January 2009.
15. Yuasa, S.; Zhu, Y.; Sogo, S. Ignition and Combustion of Aluminum in Oxygen/Nitrogen Mixture Streams. *Combust. Flame* **1997**, *108*, 387–390. [[CrossRef](#)]
16. Yuasa, S.; Zhu, Y. Effects of Oxygen Concentration on Combustion of Aluminum in Oxygen/Nitrogen Mixture Streams. *Combust. Flame* **1998**, *115*, 327–334.
17. Huang, Y.; Risha, G.A.; Yang, V.; Yetter, R.A. Effect of Particle Size on Combustion of Aluminum Particle Dust in Air. *Combust. Flame* **2009**, *156*, 5–13. [[CrossRef](#)]
18. Meinkohn, D. The Effect of Particle Size and Ambient Oxidizer Concentration on Metal Particle Ignition. *Combust. Sci. Technol.* **2009**, *181*, 1007–1037. [[CrossRef](#)]
19. Bui, D.T.; Chan, M.L.; Atwood, A.I.; AtienzaMoore, T.M.; Curran, P.O.; Turner, A.D. Combustion Behaviors of Aluminized Propellants in PCP Binder. In Proceedings of the 51st JANNAF Propulsion Meeting, Lake Buena Vista, FL, USA, 19–21 November 2002.
20. Height, J.L.; Donaldson, A.B.; Gill, W.; Parigger, C.G. Measurements in Solid Propellant Plumes at Ambient Conditions. In Proceedings of the ASME International Mechanical Engineering Congress and Exposition, IMECE2011, Denver, CO, USA, 11–17 November 2011.
21. Coker, E.N.; Donaldson, B.; Gill, W.; Yilmaz, N.; Vigil, F.M. The Isothermal Oxidation of High-Purity Aluminum at High Temperature. *Appl. Sci.* **2023**, *13*, 229. [[CrossRef](#)]

**Disclaimer/Publisher's Note:** The statements, opinions and data contained in all publications are solely those of the individual author(s) and contributor(s) and not of MDPI and/or the editor(s). MDPI and/or the editor(s) disclaim responsibility for any injury to people or property resulting from any ideas, methods, instructions or products referred to in the content.